Journal of Molecular Structure 1189 (2019) 328–337

Contents lists available at ScienceDirect

Journal of Molecular Structure

journal homepage: http://www.elsevier.com/locate/molstruc

Synthesis, spectroscopic, X-ray diffraction and tautomeric properties of 5-(diethylamino)-2-((2-(5-(3-methyl-3-phenylcyclobutyl)-6H-1,3,4-thiadiazin-2yl)hydrazono)methyl)phenol: A combined experimental and theoretical study

Alaaddin Cukurovali [a], Tuncay Karakurt [b, *]

[a] Department of Chemistry, Faculty of Science, Firat University, 23119, Elazig, Turkey
[b] Department of Chemical and Process Engineering, Faculty of Engineering-Architecture, Kırşehir Ahi Evran University, Kirsehir, 40100, Turkey

ARTICLE INFO

Article history:
Received 25 January 2019
Received in revised form
10 April 2019
Accepted 11 April 2019
Available online 12 April 2019

Keywords:
Gaussian 09
X-ray
Tautomeric
PBC
Quantum-Espresso

ABSTRACT

In this study, 5-(diethylamino)-2-((2- (5- (3-methyl-3-phenylcyclobutyl) -6H-1,3,4-thiadiazin-2yl) hydrazono)methyl)phenol single crystal, which is Schiff base, was synthesized. The synthesized crystal structure was confirmed by X-ray diffraction, IR, ^{1}H and ^{13}C NMR spectroscopic techniques. The molecules are linked by two intermolecular (C–H···O and N–H···N) and an intramolecular (O–H···N) hydrogen bonds. It was observed that the title compound can be in two tautomeric structures. The geometric parameters, ^{13}C-, ^{1}H- NMR and IR spectra and frontier molecular orbitals (FMO) of the title crystal were optimized using the Gaussian 09 package program with DFT theory, as well as the tautomer structures were compared with the IRC (Intrinsic Reaction Coordinate) analysis method. In addition, the lattice energies of two tautomer structures were calculated by Quantum-Espresso program using periodic boundary conditions (PBC). All theoretical and experimental studies were executed on two tautomeric structures. Theoretical calculations were made to compare with experimental results.

1. Introduction

In recent years, proton transfer between atoms in molecules has been a subject of great interest due to its importance in many biological and chemical processes. Many theoretical and experimental researches have been conducted to enrich the knowledge about the potential mechanisms and properties of proton transfer and tautomeric equilibrium [1–11]. In particular, it is known that the role played by the solvent is very important [12,13].

The Schiff base compounds have N = C functional group. The Schiff bases derived from the aromatic compounds containing ortho-hydroxy group are observed that two types of intramolecular N–H···O or O–H···N hydrogen bonds. Two tautomeric structures can be formed from the OH group to the N atom or from the NH group to the O atom by proton transfer. These tautomeric structures exhibit photochromism and thermochromism properties. The photochromism features are used for measuring and controlling the intensity of radiation, as well as for imaging systems and optical computers [14]. The Schiff base are used as starting materials in the synthesis of essential drugs such as antibiotics, anti-allergic, anti-phlogistic and anti-tumor [15–17]. Schiff bases are used as corrosion inhibitors due to the C = N group in their structures [18]. Multi-threaded Schiff bases with large number donor atoms exhibit biological activity with broad spectrum and have a special place in coordination chemistry due to the binding diversity of transition metal ions. It was found that their metal complexes increased the activity of some drugs and their metal chelates stopped tumor growth [19–21]. Schiff base complexes obtained from aromatic amines are used in the field of chemotherapy as oxygen carrier to various substrates in some chemical reactions [22]. In addition, Schiff bases synthesized by the condensation of amines with active carbonyl groups have a wide range of biological activity such as antifungal, insecticidal, antiviral and herbicidal activities [23].

1,3,4-thiadiazine compounds and derivatives can be obtained by various methods [24]. These compounds have various biological activities and are highly effective. In particular, they are widely used as drug that destroys parasites, fungi, insects and harmful plants [25]. 3-Substitue tetrahydro-1,3,5-thiadiazin-2-thione derivatives have anti-protozoan and anti-tuberculosis activity as prodrugs [26,27].

* Corresponding author.
E-mail address: tuncaykarakurt@gmail.com (T. Karakurt).

https://doi.org/10.1016/j.molstruc.2019.04.052
0022-2860/

The cyclobutane ring with four-carbon enables the molecule to be in a more stable conformation by puckering. The puckering reduces the total tension by decreasing the C–C–C angles that must be present in planar molecules [28].

The title compound, which is a synthesized novel Schiff base in the light of biological effects, was confirmed by using IR, ^{1}H, ^{13}C NMR spectroscopic and X-ray diffraction analysis techniques. Some theoretical studies have been performed to support experimental studies.

2. Materials and methods

2.1. X-rays crystal structure determination

Single crystalline data were obtained using Bruker AXS APEX CCD [29] diffractometer at 296 K, using 0.71073 Å wavelength MoKα radiation. The crystal structure was solved by direct methods using SHELXT-2014 [30] and was refinement by least squares methods using the SHELXL-2014 [31].

2.2. Synthesis

A mixture of 4-diethylamino salicylaldehyde (1.9325 g, 10 mmol) and hydrazinecarbothiohydrazide (1.0615 g, 10 mmol) in 30 mL of ethanol was refluxed for 2 h (TLC). Subsequently, a solution of α-haloketone (2.2271 g, 10 mmol) in 20 mL of ethanol was added dropwise at room temperature and mixture was stirred for 3 h (TLC). After made alkaline with an aqueous solution of NH_3 (5%) to modulate pH of the solution to ≈5, a light yellow precipitate separated immediately. The precipitate was filtered off, washed with copious water several times and dried in air and crystallized from EtOH. Overall yield: 82%, melting point: 476 K. Characteristic IR bands: 3159 cm^{-1} ν(N–H), 1637 cm^{-1} ν(C=N azomethine), 1595 cm^{-1} ν(C=N thiadiazine), 1134 cm^{-1} ν(C–O), 715 cm^{-1} ν(C–S– thiadiazine). Characteristic ^{1}H NMR shifts ($CDCl_3$, δ, ppm): 1.22 (t, $j = 7.1$ Hz, 6H, $-CH_3$, on ethyl), 1.58 (s, 3H, $-CH_3$), 2.42–2.47 (m, 2H, $-CH_2-$, in cyclobutane), 2.57–2.2.62 (m, 2H, $-CH_2-$, in cyclobutane), 3.29 (s, 2H, $-CH_2-S$), 3.38–3.44 (q, $j = 7.4$ Hz, 4H, $-CH_2-$, on ethyl), 3.44–3.54 (quint, $j = 7.2$ Hz, 1H, ˃CH–, in cyclobutane), 6.21 (s, 1H, aromatic), 6.25 (s, 1H, aromatic), 7.03 (d, $j = 7.8$ Hz, 1H, aromatic), 7.16–7.22 (m, 3H, aromatics), 7.31–7.37 (m, 2H, aromatics), 8.36 (s, 1H, azomethine), 9.56 (s, 1H, –NH–), 11.50 (s, 1H, –OH). Characteristic ^{13}C NMR shifts ($CDCl_3$, δ, ppm): 160.93, 159.72, 157.19, 154.03, 151.52, 150.57, 132.55, 128.35, 125.57, 124.59, 107.53, 103.67, 98.01, 44.53, 38.92, 37.60, 34.38, 30.36, 23.25, 12.71. Scheme 1.

2.3. Computational details

The crystal structure solvation and refinement calculations were performed by Olex 2 [32] and molecular schemes by MERCURY [33]. Theoretical calculations of the tautomer structures were done by Gaussian 09 software [34] using DFT/B3LYP [35,36] theory and 6-31G (d) [37] basic set for the gas phase. The obtained results were visualized using the GaussView 5 [38] software. Calculations in the crystal phase were performed using the Quantum-Espresso 6.2 [39] package program under periodic boundary conditions. In the calculations, pseudopotential derived from form proposed by Perdew-Zunger (PZ) [40] containing the Local Density Approach (LDA) were used.

3. Results and discussion

3.1. Geometrical structure of title compound

In Fig. 1a and b, Fourier maps of two tautomeric structures are shown. This map shows that the proton excess around the atoms is red, and the proton deficiency is blue. The proton excess around the N3 atom is depicted in red color, while the proton deficiency around the N2 atom is depicted by the blue color (Fig. 1a). Accordingly, it can be said that the proton attached to the N3 atom is positioned incorrectly and that the N2 atom must be protonated. Fig. 1b shows that the proton is correctly positioned. Therefore, it can be said that the structure of form1 is more stable than fom 2.

The data collection details and refinement process of the crystal form1 are shown in Table 1 and the diagram of the crystal, which is drawn with % 20 probability ellipsoids, is showed Fig. 2a and the optimized molecule obtained by the Gaussian program is given in Fig. 2b.

As shown in Fig. 2a, $C_{25}H_{31}N_5OS$ crystal consist of A (C1A–C6A), A′(C1B–C6B) benzene, B(C7/C9–C11) cyclobutane, C(C12–C13/S1/C14/N1–N2) thiadiazine and D (C16–C21) toluene rings. Each of these rings is approximately planar and the maximum deviation values of these rings were found as 0.022, 0.028, 0.127, 0.360 and 0.018 Å respectively. Also, the dihedral angles between these rings are A/B = 40.70 (5)°, B/C = 45.10 (2)° and C/D = 22.91 (12)°. The puckering angle between C11/C7/C9 and C9/C10/C11 means in the cyclobutane ring was observed as 25.98 (2)° for form1. This puckering angle value is given in the literature as 24.7 (2)° [41]. In addition, there is rotational disorder in the benzene ring. X-ray diffraction and some calculated geometric parameters of form1 and form2 are given in Table 2.

X-ray studies were performed on form1. When the X-ray diffraction results in Table 2 were examined, it was observed that

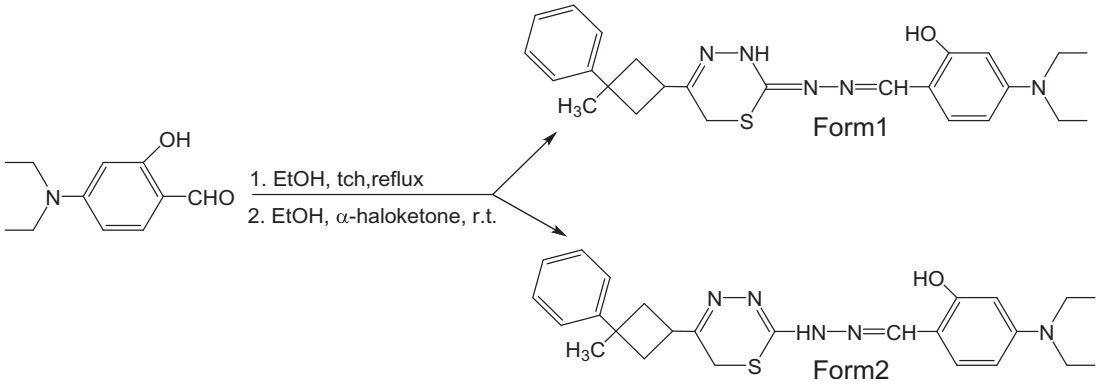

Scheme 1. The synthesis scheme of the tautomer compounds.

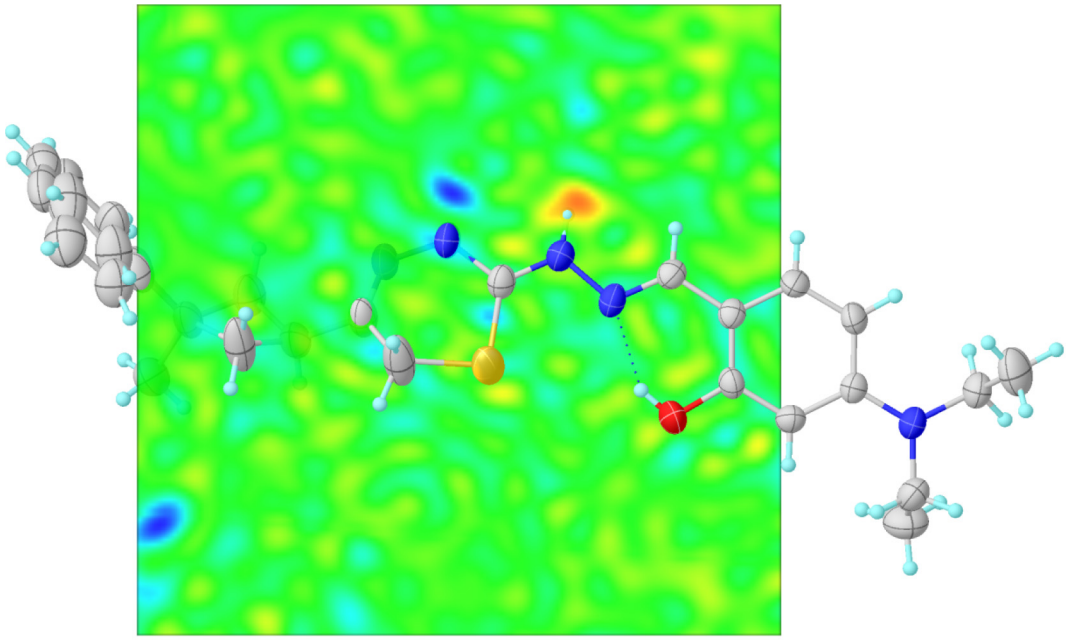

(a)

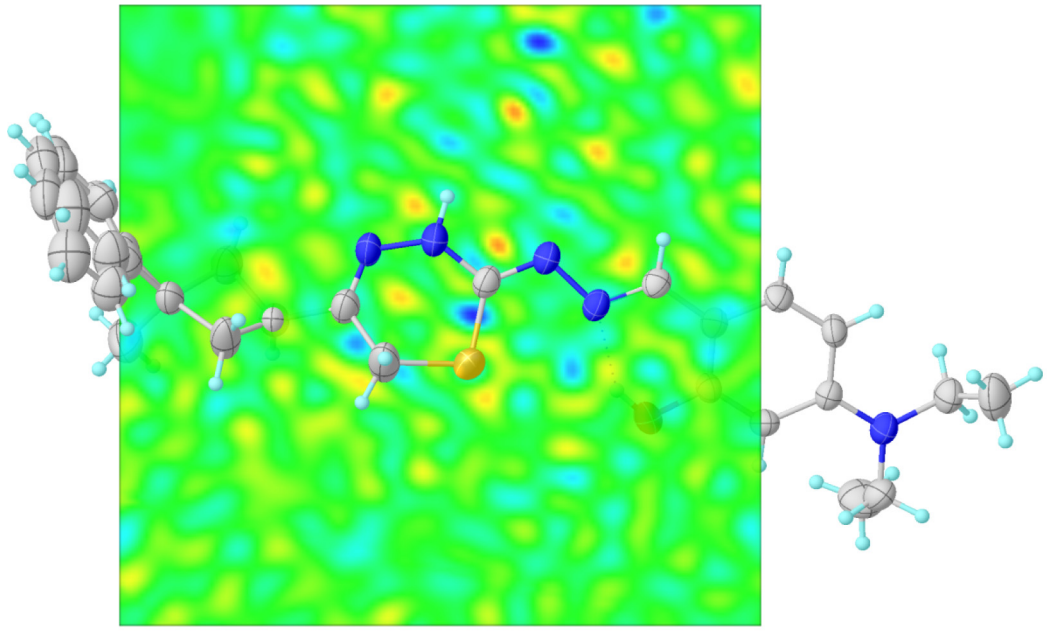

(b)

Fig. 1. Electron density map of (a) form1 (b) form2.

Table 1
Data collection and refinement values of the crystal form1.

Chemical formula	$C_{25}H_{31}N_5OS$
M_r	449.61
Temperature(K)	293 (2)
Crystal system, space group	Monoclinic, *P21/n*
a, b, c (Å)	13.514(12), 13.343(11), 14.430(13)
β (°)	103.10 (3)
V (Å^3)	2534 (4)
Z	4
ρ_{calc}g/cm^3	1.178
μ(mm^{-1})	0.153
F (000)	960.0
Crystal size (mm)	0.19 × 0.16 × 0.13
Radiation type	MoKα
2Θ range for data collection/°	5.798 to 49.998
Index ranges	$-16 \le h \le 16$, $-15 \le k \le 15$, $-17 \le l \le 17$
Reflections collected	52091
Independent reflections	4405 [Rint = 0.0547, Rsigma = 0.0284]
Data/restraints/parameters	4405/85/349
Goodness-of-fit on F^2	1.090
Final R indexes [I ≥ 2σ (I)]	R1 = 0.0636, w*R2* = 0.1264
Final R indexes [all data]	R1 = 0.0800, w*R2* = 0.1344
$\Delta\rho_{max}$, $\Delta\rho_{min}$ (e Å^{-3})	0.30, −0.23
CCDC	1888744

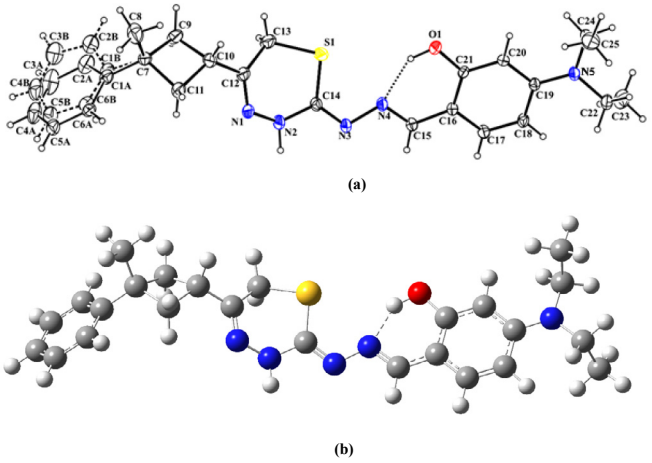

Fig. 2. (a) Experimental (b) Calculated figures of $C_{25}H_{31}N_5OS$ crystal in form1 structure.

the double bond N1=C12 and N3=C14 in the thiadiazine ring was shorter than the N2–C14 single bond length. Experimentally, these bond lengths were observed as 1.26, 1.29 and 1.37, respectively. The crystal structure was stabilized by forming the S (6) closed ring motif with O–H···N type intramolecular hydrogen bond. In addition, two intermolecular N–H···N and C–H···O classical hydrogen bonds were determined. The N2 atom (symmetry code: x, y, z), by acting as a donor, forms a N–H···N hydrogen bond with the N3 atom (symmetry code: 1-x, 1-y, 1-z). These formed hydrogen bonds generate $R_2^2(8)$ ring motif dimers. The dimers with C (18) chain motif were formed by the C–H···O type intermolecular hydrogen bond connecting C4A to O1 atoms (Fig. 3). Symmetry information of all these interactions is given in Table 3.

3.2. Tautomerizm (IRC)

We have examined two tautomer structures of the title compound by using the theoretical calculations. We have calculated some structure parameters of the transition state (TS) and two tautomer structures. The energies of form1, form2 and TS and the differences between them, activation energies of forward and reverse reactions are shown in Table 4. The image-frequency of TS was calculated as 1768i cm^{-1} and the accuracy of TS was also proved.

While the tautomeric structures transform into each other by intramolecular proton migration, some changes in the structure may occur. If we look at Table 5, while the proton transfer was carried out from form1 to form2, C14–N3 bond length and C14–N3–N4 bond angle were increased and N2–C14 bond length and N2–C14–N3 bond angle decreased.

The proton transfer process is shown in Fig. 4. The energy difference between form1 and form2 is calculated as −62.4 kj/mol and the form1 is more stable than the form2. Relative energy of TS according to the form1 was calculated as 183.91 kj/mol and the reaction energy of the reverse barrier was calculated as 121.52 kj/mol in Table 4. **ΔH (**standard enthalpy chance) and **ΔG (**free energy change) positive results indicate that the reactions processes (Form1 ↔ Form2) are endothermic and non-spontaneous at room temperature [42]. According to all these results, it can be said that the form1 is more stable than the form2 and is closer to the structure determined by X-ray.

Table 2
Experimental and calculated geometric parameters of two tautomeric structures.

Bond lengths (Å)	Experimental (Form1)	Experimental (Form2)	DFT (Form1)	DFT (Form2)
C1A–C2A	1.39 (2)	1.39 (2)	1.40	1.40
C21–O1	1.36 (3)	1.362 (3)	1.35	1.35
C2A–C3A	1.40 (2)	1.40 (2)	1.40	1.40
C3A–C4A	1.37 (2)	1.37 (2)	1.40	1.40
C4A–C5A	1.38 (2)	1.37 (2)	1.40	1.40
C14–N3	1.29 (3)	1.284 (3)	1.29	1.37
C12–N1	1.26 (4)	1.264 (4)	1.28	1.29
C14–N2	1.37 (3)	1.375 (3)	1.40	1.30
C14–S1	1.74 (3)	1.741 (3)	1.77	1.78
C13–S1	1.81 (3)	1.804 (3)	1.84	1.84
N1–N2	1.40 (3)	1.405 (3)	1.39	1.39
N3–N4	1.40 (3)	1.391 (3)	1.38	1.36
N5–C19	1.37 (3)	1.371 (3)	1.38	1.38
N5–C22	1.472 (3)	1.473 (3)	1.46	1.46
N5–C24	1.452 (4)	1.454 (4)	1.46	1.46
Bond Angles (°)				
C1A–C2A–C3A	122.35 (3)	123 (1)	121.01	121.04
C3A–C4A–C5A	120.19 (3)	120 (1)	119.44	119.43

(*continued on next page*)

Table 2 (*continued*)

Bond lengths (Å)	Experimental (Form1)	Experimental (Form2)	DFT (Form1)	DFT (Form2)
C4A–C5A–C6A	118.70 (3)	120 (1)	120.19	120.21
C7–C11–C10	90.25 (2)	90.2 (2)	89.34	89.44
N1–N2–C14	124.86 (3)	123.8 (2)	123.90	120.31
C13–S1–C14	97.32 (3)	97.3 (2)	96.08	92.15
C16–C21–O1	121.04 (3)	121.1 (2)	121.77	122.16
N5–C24–C25	113.62 (3)	113.7 (3)	113.97	113.88
Torsion angles (°)				
C15–C16–C21–O1	−4.9 (2)	−4.0 (4)	0.13	0.39
C16–C15–N4–N3	−174.14 (3)	−174.2 (2)	179.25	−179.59

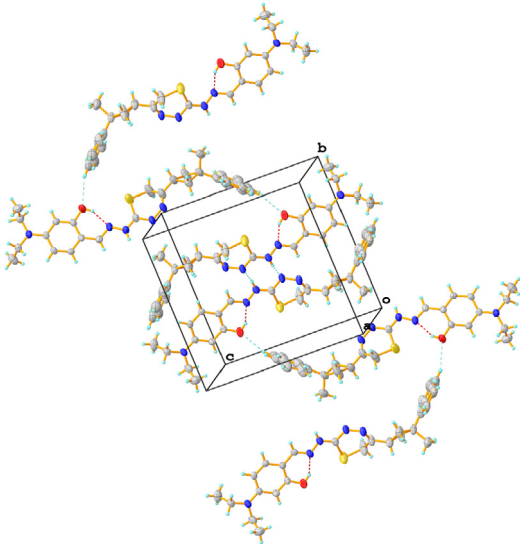

Fig. 3. Packing of crystal form1 with hydrogen bonds.

Table 3
Hydrogen Bond geometry for crystal form1 (Å, °).

D-H …. A	D-H	H …. A	D …. A	D-H …. A
O1–H1···N4	0.91 (4)	1.86 (4)	2.658 (4)	146 (4)
N2–H2···N3^{i}	0.93 (3)	2.08 (3)	3.011 (4)	175 (2)
C4A–H4A···O1^{ii}	0.93	2.59	3.455 (11)	155
C13–H13A···Cg (4) ^{iii}	0.97	2.92	3.335 (5)	107
C13–H13B···Cg (4) ^{iii}	0.97	2.93	3.335 (5)	106
C6A–H6A···Cg (4)^{iv}	0.93	2.90	3.770 (10)	156

Symmetry codes: (i) 1−x,1-y,1-z; (ii) 1/2-x, 1/2 + y, 1/2-z (iii) −1/2 + x,1/2-y,-1/2 + z; (iv) x, y,-1+z.

3.3. Periodic boundary calculations (PBC)

In the solid phase calculations, the coordinates of the atom 252 in the unit cell of the two tautomeric crystals (Figs. 5a and 6a) were used. In order to model the computational system, the change in total energy against changing plane-wave cutoff energies (E_{cut}) value was examined. As shown in Figs. 5b and 6b, E_{cut} can be

Table 5
Variation of bond lengths and angles after proton transfer process.

Bond lengths(Å)	Form1	Form2
N2–C14	1.39	1.30
C14–N3	1.29	1.37
Bond angles(°)		
C14–N3–N4	116.94	126.07
N2–C14–N3	115.70	108.18

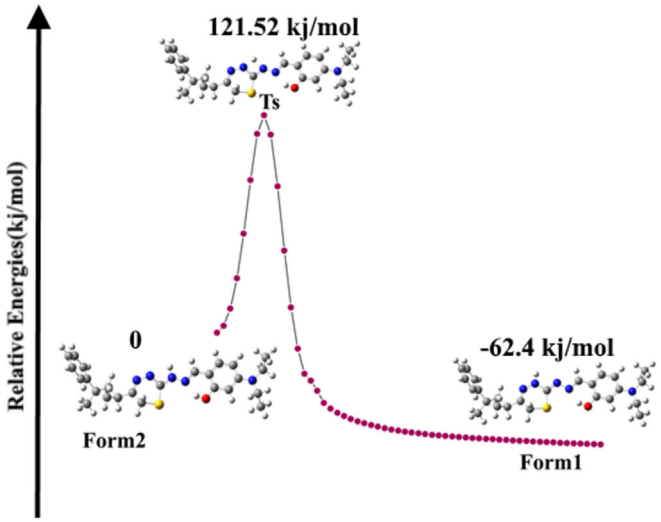

Fig. 4. Potential energy diagram for form1 and form2 structures.

neglected after the 30 Ry value. Therefore, after the 30 Ry value, all the E_{cut} make the total energy minimum. The plane-wave cutoff energies and cutoff electronic charge density were used as 80 and 160 Ry for all calculations. The k-points values were determined to be 2 × 2 × 2 and used in all calculations. The convergence criterion for energy was chosen as 10^{-7} Ry between two successive iterations. The atom coordinates of the two tautomeric structures were optimized using the vc-relax option of the Quantum-espresso program. Table 6 shows the experimental and calculated crystal parameters.

The lattice energies of the tautomeric structures were calculated

Table 4
Energies of the form1 and form2 of the title compound in hartrees, and energy differences, activation energies, and thermodynamic parameters in kJ mol^{-1}.

Form1	*Form2*	ΔE	*Ea(f)*	*Ea(r)*	$\Delta H_{298}(f)$	$\Delta G_{298}(f)$	$T\Delta S_{298}(f)$	$\Delta H_{298}(r)$	$\Delta G_{298}(r)$	$T\Delta S_{298}(r)$
−1718.4219	−1718.3981	−62.4	183.91	121.52	173.22	171.41	1.81	138.78	139.68	−0.90

$\Delta E = E_{form1}$-E_{form2}, $E_a(f)$ = forward activation energy, $E_a(r)$ = reverse activation energy.

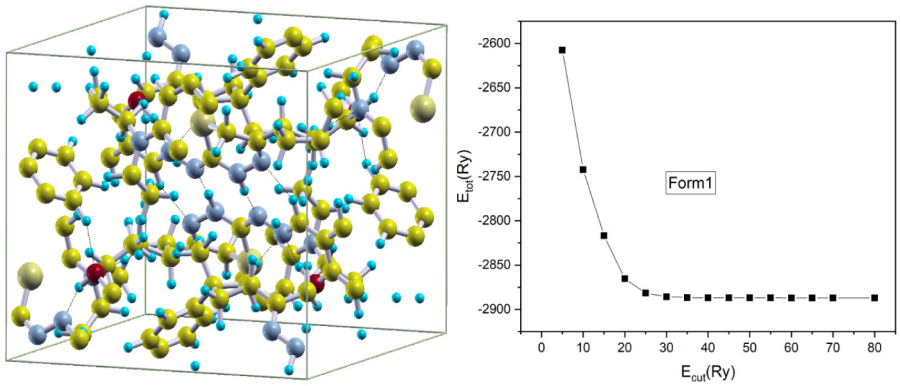

Fig. 5. (a) Representation of the atoms in the unit cell (b) energies profile of form1.

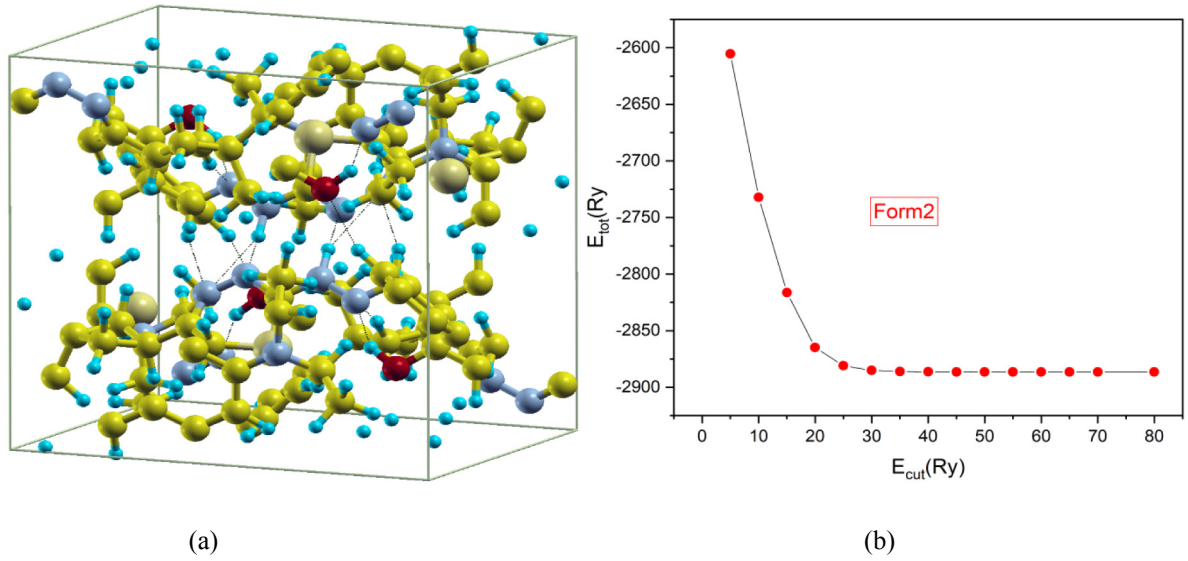

Fig. 6. (a) Representation of the atoms in the unit cell (b) energies profile of form2.

Table 6
Experimental and optimized unit cell parameters of form1 and form2.

Form1		Form2
Experimental	QE-VC-Relax/DFT	
Space group P21/n	**Space group P21/n**	**Space group P21/n**
a = 13.514 (12) Å	a = 12.654 Å	a = 12.611 Å
b = 13.343 (11) Å	b = 12.849 Å	b = 12.800 Å
c = 14.430 (13) Å	c = 14.148 Å	c = 14.184 Å
α = 90°	α = 90°	α = 90°
β = 103.10 (3)°	β = 101.89°	β = 101.96°
γ = 90°	γ = 90°	γ = 90°
Z = 4	Z = 4	Z = 4
V = 2534 (4) Å^3	V = 2251 Å^3	V = 2240 Å^3

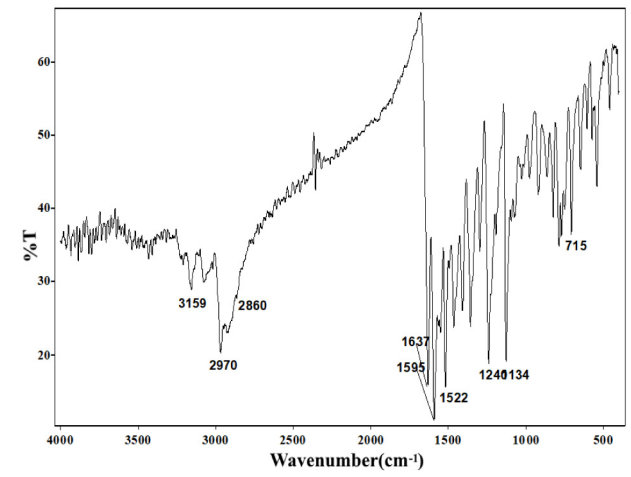

(a)

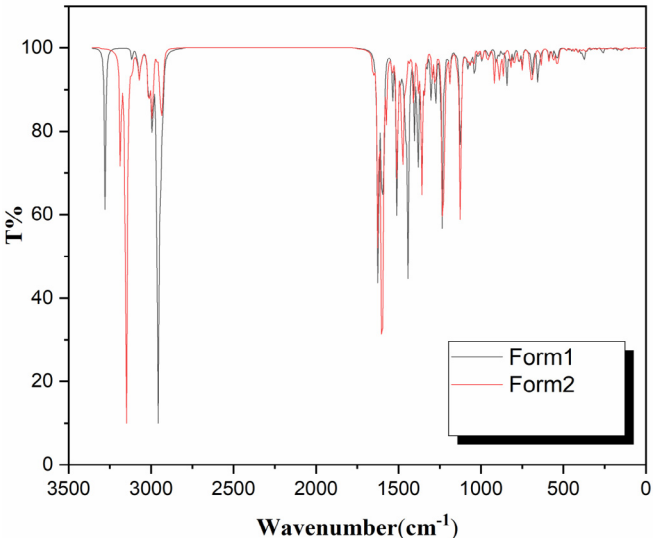

(b)

Fig. 7. (a) Experimental (b) Theoretical IR spectra of form1 and form2 structures.

using the scf option as −2887.05935080 for form1 and −2886.50624009 Ry for form2. This calculation shows that the structure of form1 is more stable.

3.4. Spectroscopic studies

The IR spectrum measured in the range 4000–400 cm^{-1} is given in Fig. 7a. Tautomeric structures have symmetric C1 symmetry containing 63 atoms in symmetric unit and 186 fundamental vibration frequencies. Theoretical calculations were made for the dimer structures of the form1 and form2. The calculated spectra of form1 and form2 structures are shown in Fig. 7b. Each frequency value is multiplied by the scale value of 0.9613 [43].

Since the proton belonging to the O–H group was used in the intra-molecular bond, this peak was not experimentally observed. This value, which is expected to be peak at the frequency between 3550 and 3200 cm^{-1} [44], is calculated as 3278 for form1 and 3186 cm^{-1} for form2. In the literature, these frequency was defined as 3436 cm^{-1} [45]. Experimentally, the proton peak belonging to the N–H group was observed at a frequency of 3159 cm^{-1}. This value is calculated as 3151 for form1 and 2957 cm^{-1} for form2 and compares well with the value reported previously [3260 cm^{-1}, 45]. Experimentally, the CS (thiadiazine), CO, C=N (thiadiazine) and C=N (azomethine) vibration frequencies were observed as 715, 1134, 1595 and 1637 cm^{-1}, respectively which have been calculated as 714, 1123, 1600 and 1600 cm^{-1} for the form1, as 714, 1126, 1599 and 1653 cm^{-1} for the form2.

The ^{1}H and ^{13}C NMR spectra (Fig. 8a) were recorded on a Varian-Gemini 400 MHz spectrometer. To determine the NMR chemical shift values of the molecules, GIAO [46,47] method was used and TMS was taken as reference. The ^{1}H and ^{13}C NMR chemical shift values calculated for the TMS by selecting the chloroform ($CDC1_3$) solvent are found as 32.16 and 189.39 ppm, respectively. Theoretical calculations were performed using dimer structures.

When the ^{13}C NMR spectrum (Fig. 8b) was examined, the chemical shifts of C14 and C21 atoms were observed as 159.72 and 160.93 ppm due to neighbor electronegative atoms (N, S and O atoms). These two chemical shift values were calculated as 153.93 and 153.59 ppm for form1, 146.62 and 152.30 ppm for form2. In the ^{1}H NMR spectrum, while the hydrogen group of the hydroxy group was experimentally observed at 11.50 ppm, this peak was calculated as 9.72 for form1 and 9.27 ppm for form2. Experimentally, the proton peak of the azomethine group was observed at 8.36 ppm and was calculated as 8.02 for form1 and 7.8 ppm for form2. While the frequency of NH group was measured as 9.56 ppm, the peak was calculated 10.92 for form1 and 11.69 ppm for form2. These results of IR and NMR calculation have shown that the structure of form1 was more consistent with the experimental results.

3.5. Frontier molecular orbitals

The orbitals called HOMO and LUMO are the most important energy levels in molecular system. These orbitals determine electron donating affinity and electron withdrawing affinity. The energy difference between these two orbitals has an important role in determining the molecular electrical transport properties. Therefore, it is largely responsible for determining chemical stability and spectroscopic properties of molecules [48]. In addition, it was stated that the biological activity of the large HOMO energy value was higher in the study previously studied [40,41]. The HOMO and LUMO energy values were −4.61 and −0.97 eV for form1, respectively, while −4.57 and −1.01 eV for form2. As shown in Fig. 9, HOMO and LUMO localized orbitals on thiadiazine, azomethine and toluene groups of dimer molecules. When $\Delta E = E_{LUMO}\text{-}E_{HOMO}$ energy intervals of the tautomeric structures were examined, it was calculated 3.64 for form1 structure and 3.56 eV for form2. As a result, it can be said that the structure of form1 has a more stable structure due to the energy difference is larger [41].

4. Conclusions

In this study, the structure of 5-(diethylamino)-2-((2-(5-(3-methyl-3-phenylcyclobutyl)-6H-1,3,4-thiadiazin-2yl)hydrazono) methyl)phenol compound is synthesized and characterized by X-ray diffraction, IR and NMR spectroscopic methods. In the experimental and theoretical studies, form1 structure was found to be more stable than form2. In the light of all the results, it was seen

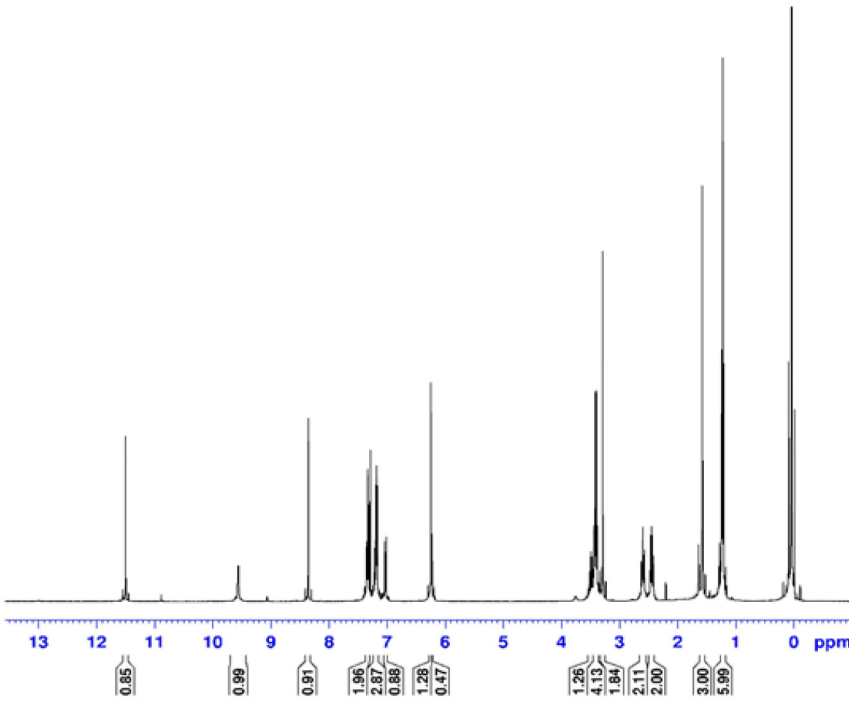

(a)

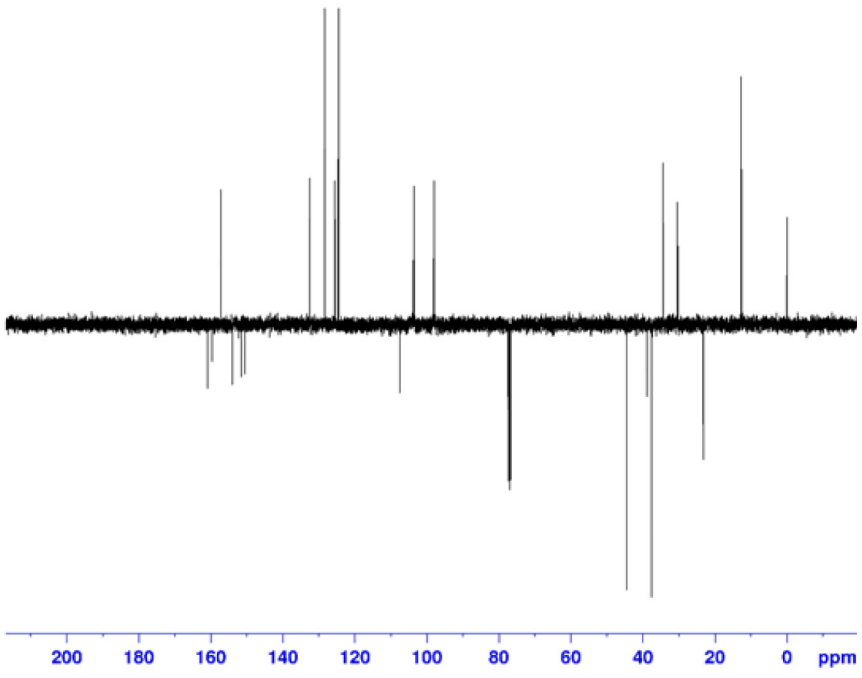

(b)

Fig. 8. (a) ^{1}H and (b) ^{13}C experimental spectra of form1 structure.

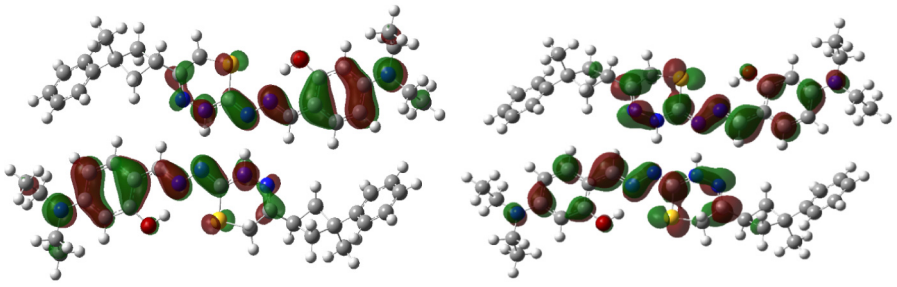

HOMO (-4.61 eV) LUMO (-0.97 eV)

(a)

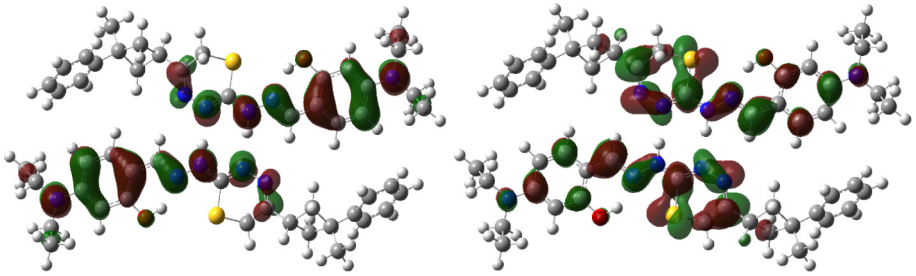

HOMO (-4.57 eV) LUMO(-1.01 eV)

(b)

Fig. 9. Molecular orbital surfaces and energy levels for the HOMO and LUMO of (a) form1 and (b) form2 structures.

that experimental and theoretical calculations were compatible.

Acknowledgement

Computing resources used in this work were provided by the National Center for High Performance Computing of Turkey (UHeM) under grant number (5005172018).

References

[1] G.R. Desiraju, The CH. cntdot.. cntdot.. cntdot. O hydrogen bond in crystals: what is it? Acc. Chem. Res. 24 (10) (1991) 290–296.
[2] E.G. Robertson, J.P. Simons, Getting into shape: conformational and supramolecular landscapes in small biomolecules and their hydrated clusters, Phys. Chem. Chem. Phys. 3 (1) (2001) 1–18.
[3] Y.-Q. Wang, H.-G. Wang, S.-Q. Zhang, K.-M. Pei, X. Zheng, D. Lee Phillips, Resonance Raman intensity analysis of the excited state proton transfer dynamics of 2-nitrophenol in the charge-transfer band absorption, J. Chem. Phys. 125 (21) (2006) 214506.
[4] D.-S. Ahn, S. Lee, B. Kim, Solvent-mediated tautomerization of purine: single to quadruple proton transfer, Chem. Phys. Lett. 390 (4–6) (2004) 384–388.
[5] K.C. Hunter, L.R. Rutledge, S.D. Wetmore, The hydrogen bonding properties of cytosine: a computational study of cytosine complexed with hydrogen fluoride, water, and ammonia, J. Phys. Chem. A 109 (42) (2005) 9554–9562.
[6] A. Douhal, S. Kim, A. Zewail, Femtosecond molecular dynamics of tautomerization in model base pairs, Nature 378 (6554) (1995) 260.
[7] A.L. Sobolewski, W. Domcke, Ab initio study of the excited-state coupled electron–proton-transfer process in the 2-aminopyridine dimer, Chem. Phys. 294 (1) (2003) 73–83.
[8] T. Schultz, E. Samoylova, W. Radloff, I.V. Hertel, A.L. Sobolewski, W. Domcke, Efficient deactivation of a model base pair via excited-state hydrogen transfer, Science 306 (5702) (2004) 1765–1768.
[9] A. Bach, C. Tanner, C. Manca, H.-M. Frey, S. Leutwyler, Ground-and excited state proton transfer and tautomerization in 7-hydroxyquinoline·(NH 3) n clusters: spectroscopic and time resolved investigations, J. Chem. Phys. 119 (12) (2003) 5933–5942.
[10] M. Meuwly, A. Bach, S. Leutwyler, Grotthus-type and diffusive proton transfer in 7-hydroxyquinoline⊙(NH3) n clusters, J. Am. Chem. Soc. 123 (46) (2001) 11446–11453.
[11] R. Casadesús, M. Moreno, J.M. Lluch, A theoretical study of the ground and first excited singlet state proton transfer reaction in isolated 7-azaindole–water complexes, Chem. Phys. 290 (2–3) (2003) 319–336.
[12] M.C.P. Lima, K. Coutinho, S. Canuto, W.R. Rocha, Reaction mechanism and tautomeric equilibrium of 2-mercaptopyrimidine in the gas phase and in aqueous solution: a combined Monte Carlo and quantum mechanics study, J. Phys. Chem. A 110 (22) (2006) 7253–7261.
[13] N. Özdemir, S. Dayan, O. Dayan, M. Dinçer, N.Ö. Kalaycıoğlu, Experimental and molecular modeling investigation of (E)-N-{2-[(2-hydroxybenzylidene) amino] phenyl} benzenesulfonamide, Mol. Phys. 111 (6) (2013) 707–723.
[14] K.H. Reddy, P.S. Reddy, P.R. Babu, Nuclease activity of mixed ligand complexes of copper (II) with heteroaromatic derivatives and picoline, Transit. Metal Chem. 25 (5) (2000) 505–510.
[15] G. Ayhan-Kılcıgil, C. Kus, E.D. Özdamar, B. Can-Eke, M. Iscan, Synthesis and antioxidant capacities of some new benzimidazole derivatives, Arch. Pharm. 340 (11) (2007) 607–611.
[16] M.J. O'Neil, A. Smith, P. Heckelman, The Merck Index, thirteenth ed., Merck & Co, Inc., Whitehouse Station, NJ 6596, 2001.
[17] C. Kus, G. Ayhan-Kilcigil, B.C. Eke, Synthesis and antioxidant properties of some novel benzimidazole derivatives on lipid peroxidation in the rat liver, Arch Pharm. Res. (Seoul) 27 (2) (2004) 156.
[18] P.J. Blower, Small coordination complexes as radiopharmaceuticals for cancer targeting, Transit. Metal Chem. 23 (1) (1997) 109–112.
[19] F. Dwyer, E. Mayhew, E. Roe, A. Shulman, Inhibition of landschuetz ascites tumour growth by metal chelates derived from 3, 4, 7, 8-tetramethyl-1, 10-phenanthroline, Br. J. Canc. 19 (1) (1965) 195.
[20] A.A. El-Sherif, T.M. Eldebss, Synthesis, spectral characterization, solution equilibria, in vitro antibacterial and cytotoxic activities of Cu (II), Ni (II), Mn (II), Co (II) and Zn (II) complexes with Schiff base derived from 5-bromosalicylaldehyde and 2-aminomethylthiophene, Spectrochim. Acta Mol. Biomol. Spectrosc. 79 (5) (2011) 1803–1814.
[21] C. Jayabalakrishnan, K. Natarajan, Ruthenium (II) carbonyl complexes with tridentate Schiff bases and their antibacterial activity, Transit. Met. Chem. 27 (1) (2002) 75–79.
[22] M.E. Mahmoud, M.M. El-Essawi, S.A. Kholeif, E.M. Fathalla, Aspects of surface modification, structure characterization, thermal stability and metal selectivity properties of silica gel phases-immobilized-amine derivatives, Anal. Chim. Acta 525 (1) (2004) 123–132.
[23] L. Li, Z. Li, K. Wang, Y. Liu, Y. Li, Q. Wang, Synthesis and antiviral, insecticidal, and fungicidal activities of gossypol derivatives containing alkylimine, oxime or hydrazine moiety, Bioorg. Med. Chem. 24 (3) (2016) 474–483.
[24] N. Nami, F. Gholami, H. Vahedi, N.J.P. Nami, Sulfur, silicon, synthesis of thiadiazine and triazino [3, 4-b] thiadiazine derivatives, Phosphorus, Sulfur, Silicon Related Elements 182 (9) (2007) 2157–2162.

[25] C. Tomalin, The Pesticide Manual Incorporation the Agrochemical Handbook, Corp Protection Council and the Royal Society of Chemistry, Protection of Publication of British, vol. 279, 1997.
[26] T. Aboul-Fadl, K. Hassanin, Tetrahydro-2H-1,3,5-thiadiazin-5-(4-pyridylcarboxamide)-2-thione. Derivatives as prodrugs for isoniazid, synthesis, investigations and InVitro antituberculous activity, Pharmazie 54 (4) (1999) 244–247.
[27] C. Ochoa, E. Pérez, R. Pérez, M. Suárez, E. Ochoa, H. Rodrigez, A.G. Barrio, M. Susana, J.J. Nogal, R.A. Martinez, Synthesis and antiprotozoan properties of new 3,5-disubstituted-tetrahydro-2H-1,3,5-thiadiazine-2-thione derivatives, Arzneim. Forsch. Drug Res. 49 (9) (1999) 764–769.
[28] H. Hart, D.J. Hart, L.E. Craine, Organic Chemistry-A Short Course, Houghton Mifflin Company, 1995.
[29] A. Bruker, APEX2, V2008. 6, SADABS V2008/1, SAINT V7. 60A, SHELXTL V6. 14, Bruker AXS Inc., Madison, Wisconsin, USA, 2008.
[30] G.M. Sheldrick, SHELXT–Integrated space-group and crystal-structure determination, Acta Crystallogr. A: Found. Adv. 71 (1) (2015) 3–8.
[31] G.M. Sheldrick, Crystal structure refinement with SHELXL, Acta Crystallogr. C: Struct. Chem. 71 (1) (2015) 3–8.
[32] O.V. Dolomanov, L.J. Bourhis, R.J. Gildea, J.A. Howard, H. Puschmann, OLEX2: a complete structure solution, refinement and analysis program, J. Appl. Crystallogr. 42 (2) (2009) 339–341.
[33] C.F. Macrae, I.J. Bruno, J.A. Chisholm, P.R. Edgington, P. McCabe, E. Pidcock, L. Rodriguez-Monge, R. Taylor, J.v.d. Streek, P.A. Wood, New features for the visualization and investigation of crystal structures, J. Appl. Crystallogr. 41 (2) (2008) 466–470.
[34] M. Frisch, G. Trucks, H.B. Schlegel, G. Scuseria, M. Robb, J. Cheeseman, G. Scalmani, V. Barone, B. Mennucci, G. Petersson, Gaussian 09, Revision a. 02, gaussian, Inc., Wallingford, CT 200, 2009.
[35] A.D. Becke, Density-functional thermochemistry. III. The role of exact exchange, J. Chem. Phys. 98 (7) (1993) 5648–5652.
[36] C. Lee, W. Yang, R.G. Parr, Development of the Colle-Salvetti correlation-energy formula into a functional of the electron density, Phys. Rev. B 37 (2) (1988) 785.
[37] J.B. Foresman, A. Frisch, Exploring Chemistry with Electronic Structure Methods: a Guide to Using Gaussian, 1996.
[38] R. Dennington, T. Keith, J. Millam, K. Eppinnett, W.L. Hovell, R. Gilliland, GaussView, Version, 2009.
[39] P. Giannozzi, S. Baroni, N. Bonini, M. Calandra, R. Car, C. Cavazzoni, D. Ceresoli, G.L. Chiarotti, M. Cococcioni, I. Dabo, Quantum Espresso: a modular and open-source software project for quantum simulations of materials, J. Phys. Condens. Matter 21 (39) (2009), 395502.
[40] J. Perdew, J.P. Perdew, A. Zunger, Phys. Rev. B 23 (1981) 5048.
[41] T. Karakurt, Investigation of the molecular structure of 4-(3-methyl-3-phenylcyclobutyl)-2-[2-(3-methylbenzylidene) hydrazinyl] thiazole in the gas and solid phases, Acta Crystallogr. C74 (11) (2018) 1502–1508.
[42] R.N. Singh, Vikas Baboo, Poonam Rawat, Kumar Amit, Divya Verma, Molecular structure, spectral studies, intra and intermolecular interactions analyses in a novel ethyl 4-[3-(2-chloro-phenyl)-acryloyl]-3,5-dimethyl-1 H-pyrrole-2-carboxylate and its dimer: a combined DFT and AIM approach, Spectrochim. Acta, Part A 94 (2012) 288–301.
[43] J.P. Merrick, D. Moran, L. Radom, An evaluation of harmonic vibrational frequency scale factors, J. Phys. Chem. A 111 (2007) 11683–11700.
[44] T. Karakurt, A. Cukurovali, N.T. Subasi, A. Onaran, A. Ece, S. Eker, I.J.C.P.L. Kani, Experimental and theoretical studies on tautomeric structures of a newly synthesized 2, 2′(hydrazine-1, 2-diylidenebis (propan-1-yl-1-ylidene)) diphenol, J. Mol. Struct. 693 (2018) 132–145.
[45] T. Karakurt, A. Cukurovali, N.T. Subasi, I. Kani, Molecular structure and computational studies on 2-((2-(4-(3-(2, 5-dimethylphenyl)-3-methylcyclobutyl) thiazol-2-yl) hydrazono) methyl) phenol monomer and dimer by DFT calculations, J. Mol. Struct. 1125 (2016) 433–442.
[46] R. Ditchfield, Molecular orbital theory of magnetic shielding and magnetic susceptibility, J. Chem. Phys. 56 (1972) 5688–5691.
[47] P. Pulay, K. Wolinski, J. Hinton, The 3–21+ G basis set for first row elements, J. Am. Chem. Soc. 112 (1990) 8251–8260.
[48] P.W. Atkins, J. De Paula, Atkins' Physical Chemistry, 2010.